

Article

Experimental Investigation on Mechanics and Seepage Characteristics of Tectonic and Intact Coal Containing Gas

Chaolin Zhang ^{1,2,*} , Enyuan Wang ^{1,2}, Jiang Xu ³ and Shoujian Peng ^{3,*} 

¹ Key Laboratory of Gas and Fire Control for Coal Mines, China University of Mining and Technology, Xuzhou 221116, Jiangsu, China; weytop@cumt.edu.cn

² School of Safety Engineering, China University of Mining and Technology, Xuzhou 221116, Jiangsu, China

³ State Key Laboratory of Coal Mine Disaster Dynamics and Control, Chongqing University, Chongqing 400030, China; jiangxu@cqu.edu.cn

* Correspondence: chaolinzhang@cumt.edu.cn (C.Z.); sjpeng@cqu.edu.cn (S.P.); Tel.: +86-178-5117-4579 (C.Z.); +86-186-8087-1822 (S.P.)

Received: 15 September 2020; Accepted: 16 October 2020; Published: 18 October 2020



Abstract: Coalbed methane is a double-edged sword with two attributes of energy and hazard in coal mines. Gas drainage is the most direct and effective measure for gas recovery and disaster prevention in coal mines, which is seriously affected by the mechanics and seepage characteristics of coal. In this work, we experimentally simulated the triaxial compression and gas depletion processes using both tectonic coal and intact coal. The mechanics and seepage characteristics of tectonic and intact coal under the coupling effect of stress and gas pressure were analyzed and compared. The results show that during the triaxial compression, the damage stress and peak stress of tectonic coal is only half that of intact coal, while their compaction stress or residual stress are almost the same. Meanwhile, the permeability recovery value after tectonic coal failure is very limited, even smaller than that of intact coal, although its primary permeability is much larger than that of intact coal. On the contrary, the permeability recovery value after intact coal failure is more than twice of its primary permeability. During the gas depletion, the rebound gas pressure of tectonic coal is smaller than that of intact coal, and the permeability of tectonic coal is one order of magnitude larger than that of intact coal before the gas pressure drops to 2 MPa. The broken of tectonic coal and the low permeability of intact coal may be the two principal reasons. Therefore, in the tectonic coal area, the gas extraction time at high gas pressure stage should be stabilized, while in the intact coal area, the gas extraction time at low gas pressure stage should be increased, and the coal permeability enhancement measures should be combined to achieve the goal of high and stable production of coalbed methane.

Keywords: mechanical properties; seepage characteristics; tectonic coal; intact coal; coal permeability

1. Introduction

Coalbed methane (CBM, hereinafter referred to as gas) is a methane-rich gas that exists in coal and is not only a kind of high-quality clean energy, but also a serious hazard in coal mines [1–3]. Gas extraction is the most direct and effective measure for gas recovery and gas disaster control in coal mines [4]. The permeability of most coal seams in China ranges from 1.974×10^{-18} to 1.579×10^{-14} m², which is three to four orders of magnitude lower than that of most countries in the world [5–7]. Meanwhile, coal is a porous organic rock, which can be divided into tectonic coal and intact coal [8]. The tectonic coal is usually seriously broken or pulverized affected by faults, folds, slippage, and other tectonic actions, which is widely distributed in many countries, especially in China, and is considered as the principal reason of coal and gas outburst for a long time [9–11]. Relative to tectonic coal, the intact

coal retains its original structure and has different properties. Therefore, the mechanical properties and seepage characteristics of coal containing gas have an important impact on the efficiency of methane extraction and the safety production of coal mines.

Numerous researchers have conducted studies on geomechanical properties and seepage characteristics of tectonic and intact coal. Jiang and Ju [12] studied the structure and petrophysical features of tectonic coal. Li et al [13] analyzed the pore size distribution of tectonically deformed coal. Skoczylas studied the mechanical and gaseous properties of coal briquettes in terms of outburst risk [14]. Quosay et al. [15,16] proposed a new uncertainty based modeling approach for process design using Monte Carlo simulation technique in hydraulic fracturing technology to enhance gas recovery. Chaturvedi et al. [17] investigated the air–water seepage in briquette coal. Zhang et al. [18,19] studied the stress–permeability behavior of single persistent fractured coal samples in the fractured zone. Chen et al. [20] carried out gas depressurization extraction experiments using tectonic coal and analyzed the evolution of permeability and deformation of coal during gas depletion. Zhang et al. [21,22] conducted physical simulation of gas extraction using large-scale tectonic coal and explored the law of coal gas pressure, temperature, permeability, and gas flow rate. Yin et al. [23,24] investigated the geomechanical properties of intact coal with loading axial stress and unloading confining pressure. Liu et al. [25] pointed that the effective vertical stress of intact coal rose during gas depletion, while the effective horizontal stress shown various trend for different gases. Lu et al. [26] explored the gas desorption characteristics of the high-rank tectonic coal and intact coal, which shown that the broken surfaces of intact coal were relatively flat while the surfaces of tectonic coal had more sub-micron particles. Dong et al. [27] studied the mechanical properties of intact coal and tectonic coal by compression of a single particle and found that the intact coal shown obvious brittleness, whereas the tectonic coal was less brittle. Liu et al. [28] analyzed the acoustic emission in uniaxial compression of tectonic and intact coal, which can guide the prediction and prevention of coal mine disasters.

Although a lot of work has been done on the mechanical and seepage properties of tectonic coal and intact coal, the comparison between the two kinds of coal samples is relatively less, especially under the coupling effect of in situ stress and gas pressure. In this study, the experiments of triaxial compression and gas depletion using both tectonic coal and intact coal were carried out. The mechanical properties and seepage characteristics of tectonic coal and intact coal under the combined influence of stress and gas pressure were analyzed and compared.

2. Experimental Method

2.1. Experimental Apparatus

The experiments were conducted using a triaxial servo-controlled seepage device for hot-fluid–solid coupling of coal containing gas, which was developed by Chongqing University, China [29]. The apparatus consists of a triaxial chamber, a servo loading system, a water bath system, a seepage control system, and a data acquisition system, as shown in Figure 1. The maximum axial pressure, maximum confining pressure, and the maximum gas pressure provided by the apparatus is 100 MPa, 10 MPa, and 6 MPa, respectively. The mechanics and seepage characteristics of coal containing gas under different simulation conditions can be tested.

2.2. Experimental Samples

The tectonic raw coal and intact raw coal were collected from Jinjia Coal mine and Songhe Coal mine, respectively, which are all located in Southwest Guizhou Province in China. The proximate analysis of the coal samples was carried out according to the Chinese National Standard GB/T 212-2008 guidelines [30], which shows that the ash yield and volatile matter of tectonic coal are only half that of intact coal, as shown in Table 1.

Figure 2 shows the manufacturing processes of coal samples. The raw coal was initially drilled as the coal cores. Then the coal cores were cut and polished into cylindrical samples of $\Phi 50 \text{ mm} \times 100 \text{ mm}$

for experiments. The broken surfaces of intact coal samples were very flat, while there were many irregular cracks on the tectonic coal surfaces.

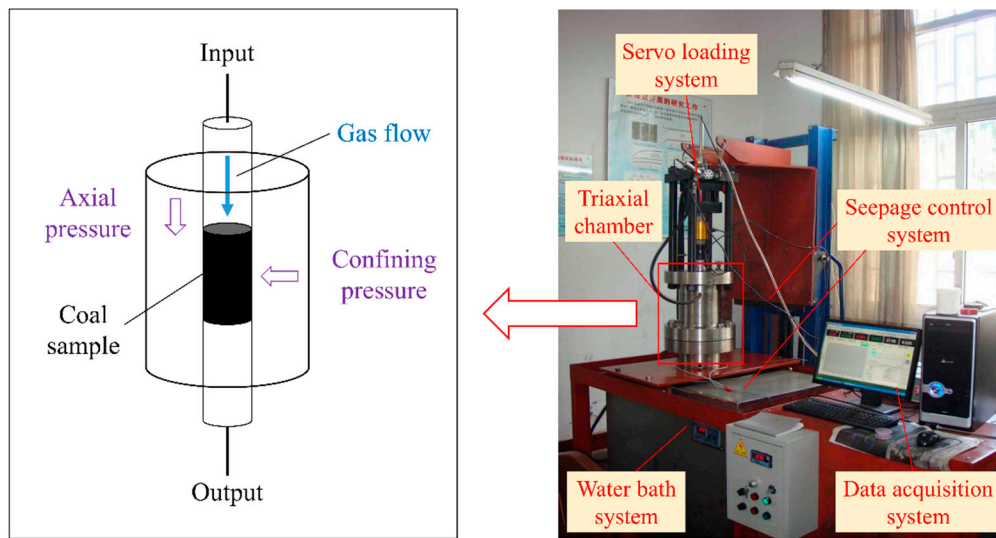


Figure 1. Experimental apparatus for mechanical-seepage coupling experiments.

Table 1. Proximate analysis of coal samples.

Coal Sample	Moisture Content, M_{ad} (%)	Ash Yield, A_{ad} (%)	Volatile Matter, V_{ad} (%)	Fixed Carbon, FC_{ad} (%)
Tectonic coal	1.82	8.20	9.06	80.92
Intact coal	1.34	15.60	19.24	63.82

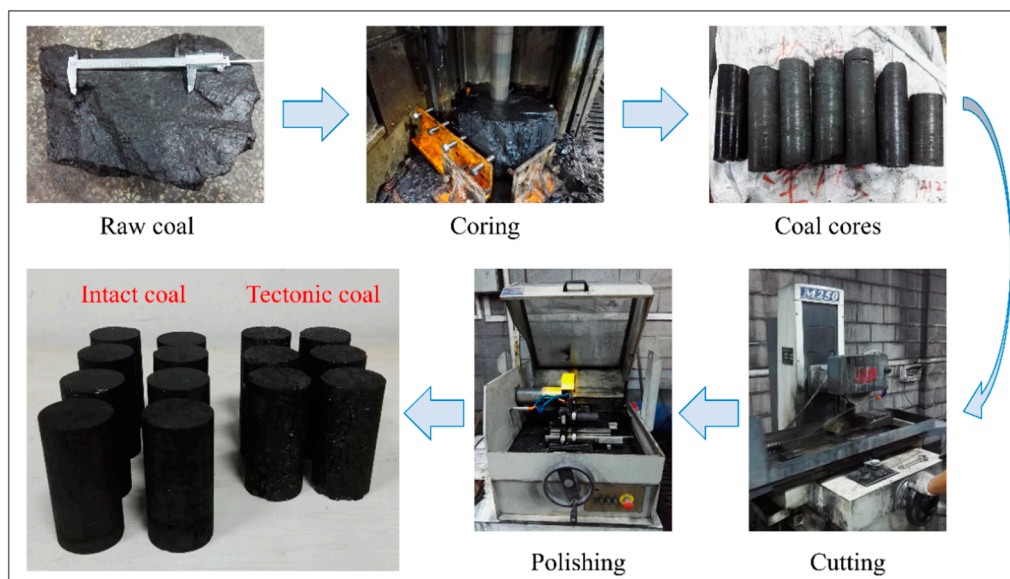


Figure 2. Manufacturing processes of coal samples.

2.3. Experimental Procedures

To obtain the mechanics and seepage characteristics of coal, two types of tests using tectonic and intact coal samples in this study, namely triaxial compression tests and gas depletion tests.

- Triaxial compression tests.

1. The coal sample surface was coated with a layer of 704 silica gel except for both ends and covered by a thermoplastic tube. Then the coal sample was placed into the triaxial chamber and the environmental temperature was set as 25 °C.
 2. After the sealing of the coal sample, the triaxial chamber was vacuumed for 12 h to remove the residual air.
 3. Applied the axial pressure of 8 MPa, the confining pressure of 4 MPa, and the gas (using pure CH₄) pressure of 1 MPa to the coal sample.
 4. The axial stress was continuously loaded by a displacement control at a speed of 0.2 mm/min until the coal sample failure while the confining pressure and the gas pressure were fixed. Monitored the axial pressure, displacement, and gas flow rate during the entire test process.
- Gas depletion tests. Steps (1) and (2) were the same as the triaxial compression tests.
 - 3 Applied the axial pressure of 12 MPa, the confining pressure of 4 MPa, and the gas (using pure CH₄) pressure of 4 MPa to the coal sample, then recorded the displacement and gas flow rate.
 - 4 Closed the gas input valve and opened the gas output valve while the axial pressure and the confining pressure were fixed. When the gas pressure was balanced at 3.5 MPa, recorded the displacement and gas flow rate. Then tested the relative data when the gas pressure was balanced at 3 MPa, 2.5 MPa, 2 MPa, 1.5 MPa, 1 MPa, and 0.5 MPa in turn.

According to the measured data in the experiments, the deviatoric stress, effective stress, and permeability of coal can be obtained as

$$\Delta\sigma = \sigma_1 - \sigma_3 \quad (1)$$

$$\sigma_0 = \frac{\sigma_1 + 2\sigma_3}{3} - \frac{p_1 + p_2}{2} \quad (2)$$

$$k = \frac{2\mu qp_0L}{A(p_1^2 - p_2^2)} \quad (3)$$

where σ_1 , σ_3 , $\Delta\sigma$, and σ_0 are the axial stress, confining stress, deviatoric stress, effective stress, respectively, MPa; p_0 , p_1 , and p_2 are the standard atmospheric pressure, gas pressures at gas input, and gas pressure at gas output, respectively, MPa; k is the permeability, m²; μ is the gas dynamic viscosity, Pa·s; q is the gas flow rate, m³/s; L is the length of the coal sample, m; and A is the permeability area of the coal sample, m².

3. Results and Discussion

3.1. Mechanical Properties of Coal during Triaxial Compression

The stress-permeability-strain evolution of tectonic coal under triaxial compression is depicted in Figure 3a. According to the coal deformation trend, the entire compression process can be divided into four stages: the compaction stage (I), the linear elastic stage (II), the yielding stage (III), and the post-destruction stage (IV) [31]. During the compaction stage, the primary pores and fractures in coal are gradually compressed with the increase of deviatoric stress. As a result, the axial strain and volumetric strain increase and the permeability of coal decreases accordingly. However, the radial strain has remained approximately constant mainly due to the confinement of confining pressure. During the linear elastic stage, the primary pores and fractures in coal continue to close. The radial strain has a slight increase, and the axial strain and volumetric strain increase linearly with the increase of deviatoric stress. Moreover, the coal permeability almost drops to its minimum because of no new pores and fractures are generated [32]. During the yielding stage, the coal expands to the radial direction obviously; however, the increase rate of axial strain and volumetric strain begin to drop slowly. At the same time, the coal permeability starts to rebound due to more and more new fractures and cracks are produced with the increase of deviatoric stress. During the post-destruction stage,

the deviatoric stress decreases with the increase of the axial strain, radial strain, and volumetric strain. The coal permeability increases furtherly with forming more and more macro-cracks.

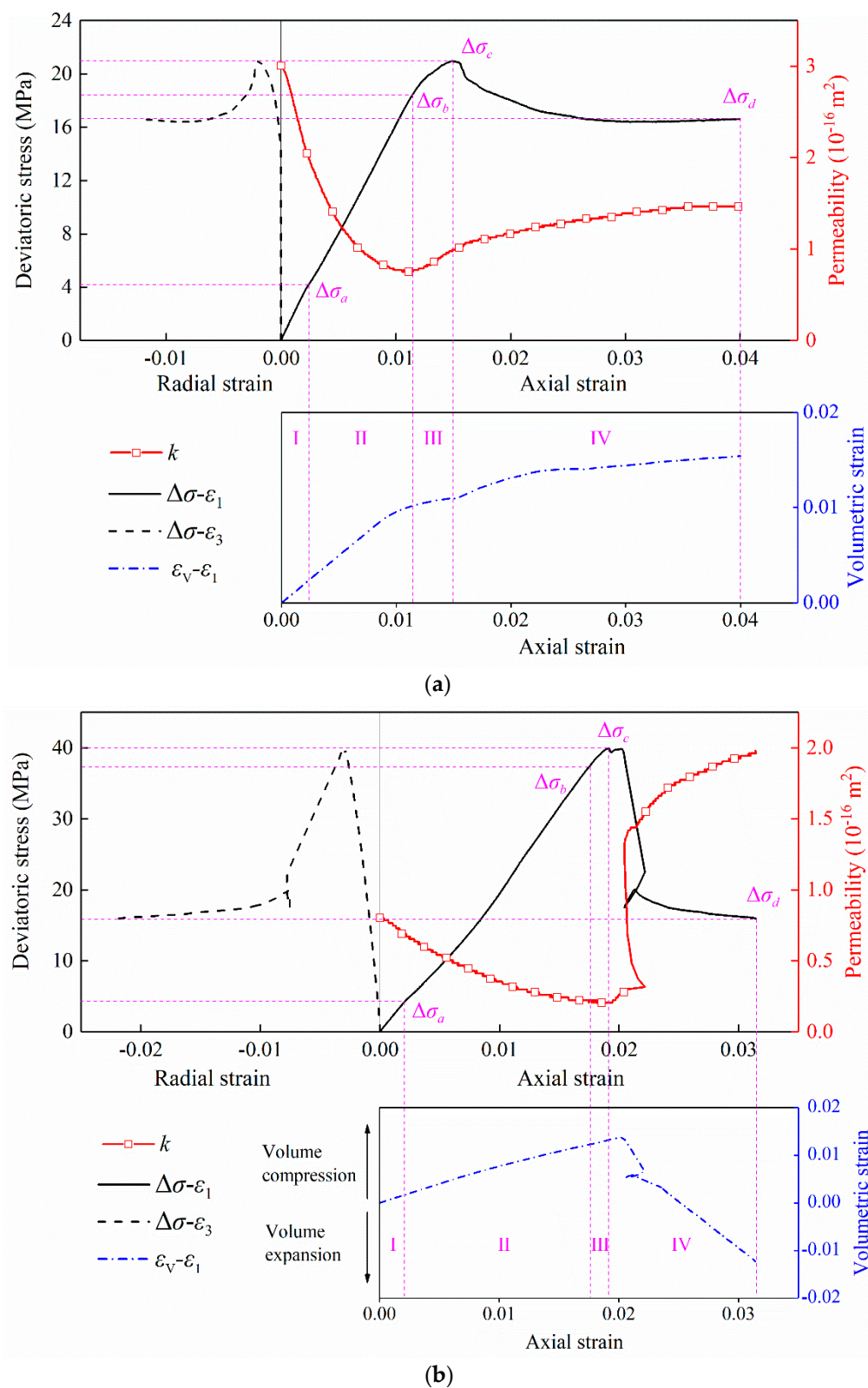


Figure 3. Stress-permeability-strain curves of coal under triaxial compression. (a) tectonic coal; (b) intact coal.

Figure 3b shows the stress-permeability-strain evolution of intact coal under triaxial compression which also can be divided into four stages. However, there are several obvious differences between two groups of stress-permeability-strain curves. Firstly, the radial strain of intact coal increases continuously from the beginning of compression, while that of tectonic coal has an apparent increase from the yielding stage. Secondly, the volumetric strain of intact coal is going down and even negative during the post-destruction stage while that of tectonic coal increases during the whole process, which means the intact coal volume has an expansion at last. Thirdly, the peak stress ($\Delta\sigma_c$) of intact coal is nearly twice as much as that of tectonic coal and the permeability of intact coal is smaller than that of tectonic coal. Eventually, the deviatoric stress of intact coal during the post-destruction stage has a sharp drop while that of tectonic coal decreases slowly which shows an apparent strain softening behavior.

In order to compare the mechanics of tectonic coal and intact coal under triaxial compression, the compaction stress ($\Delta\sigma_a$), damage stress ($\Delta\sigma_b$), peak stress, residual stress ($\Delta\sigma_d$), and the Young's modulus (E) are collected furtherly, as shown in Table 2. It can be found that the compaction stress and residual stress of tectonic coal and intact coal are almost the same, even though their damage stress or peak stress are quite different. Meanwhile, the Young's modulus of tectonic coal is only 74% that of intact coal.

Table 2. Critical stresses of tectonic and intact coal during each stage.

Coal Sample	$\Delta\sigma_a$ (MPa)	$\Delta\sigma_b$ (MPa)	$\Delta\sigma_c$ (MPa)	$\Delta\sigma_d$ (MPa)	E (GPa)
Tectonic coal	4.22	18.46	20.96	16.64	1.58
Intact coal	4.17	37.59	39.92	16.00	2.14

3.2. Seepage Lagging and Recovery Effect during Triaxial Compression

As mentioned above, during the yielding stage of triaxial compression, the coal produces new fractures and cracks leading to the increase of coal permeability. However, the rebound time of coal permeability (t_2) is later than the initial time of yielding stage (t_1), namely, the seepage lagging effect, as shown in Figure 4. The time difference of t_2 and t_1 is defined as the seepage lagging time (Δt). As we can see from Table 3, the seepage lagging time of intact coal is much larger than that of tectonic coal. Therefore, when the tectonic coal is subjected to the damage stress, its permeability increases immediately. For the intact coal subjected to the damage stress, its permeability increases after a period of time. It is mainly because that the primary fractures of tectonic coal are developed, and the new produced cracks are easy to connect the primary fractures and pass through the coal body. The new produced fractures of intact coal must reach a certain degree to pass through the coal body due to the limited primary fractures in coal.

Table 3. Critical time of tectonic and intact coal during each stage.

Coal Sample	t_1 (s)	t_2 (s)	Δt (s)
Tectonic coal	339.0	343.4	4.4
Intact coal	522.0	575.0	53.0

The permeabilities of both tectonic coal and intact coal show an evolutionary trend of decreasing first and then recovery. However, their critical permeabilities of each stage are different, as shown in Figure 4 and Table 4. The primary permeability (k_0), minimum permeability (k_1) and residual permeability (k_2) of tectonic coal and intact coal are $3.01 \times 10^{-16} \text{ m}^2$, $0.75 \times 10^{-16} \text{ m}^2$, and $1.47 \times 10^{-16} \text{ m}^2$ and $0.80 \times 10^{-16} \text{ m}^2$, $0.21 \times 10^{-16} \text{ m}^2$, and $1.96 \times 10^{-16} \text{ m}^2$, respectively. On the one hand, for the tectonic coal, the minimum permeability is only 24.9% of the primary permeability, and the residual permeability is only 48.8% of the primary permeability. For the intact coal, the minimum permeability is 26.3% of the primary permeability while the residual permeability is 245.0% of the primary permeability. On the other hand, the primary permeability and minimum permeability of tectonic coal are 3.76 times

and 3.57 times that of intact coal, respectively. However, the residual permeability of tectonic is only 75.0% that of intact coal.

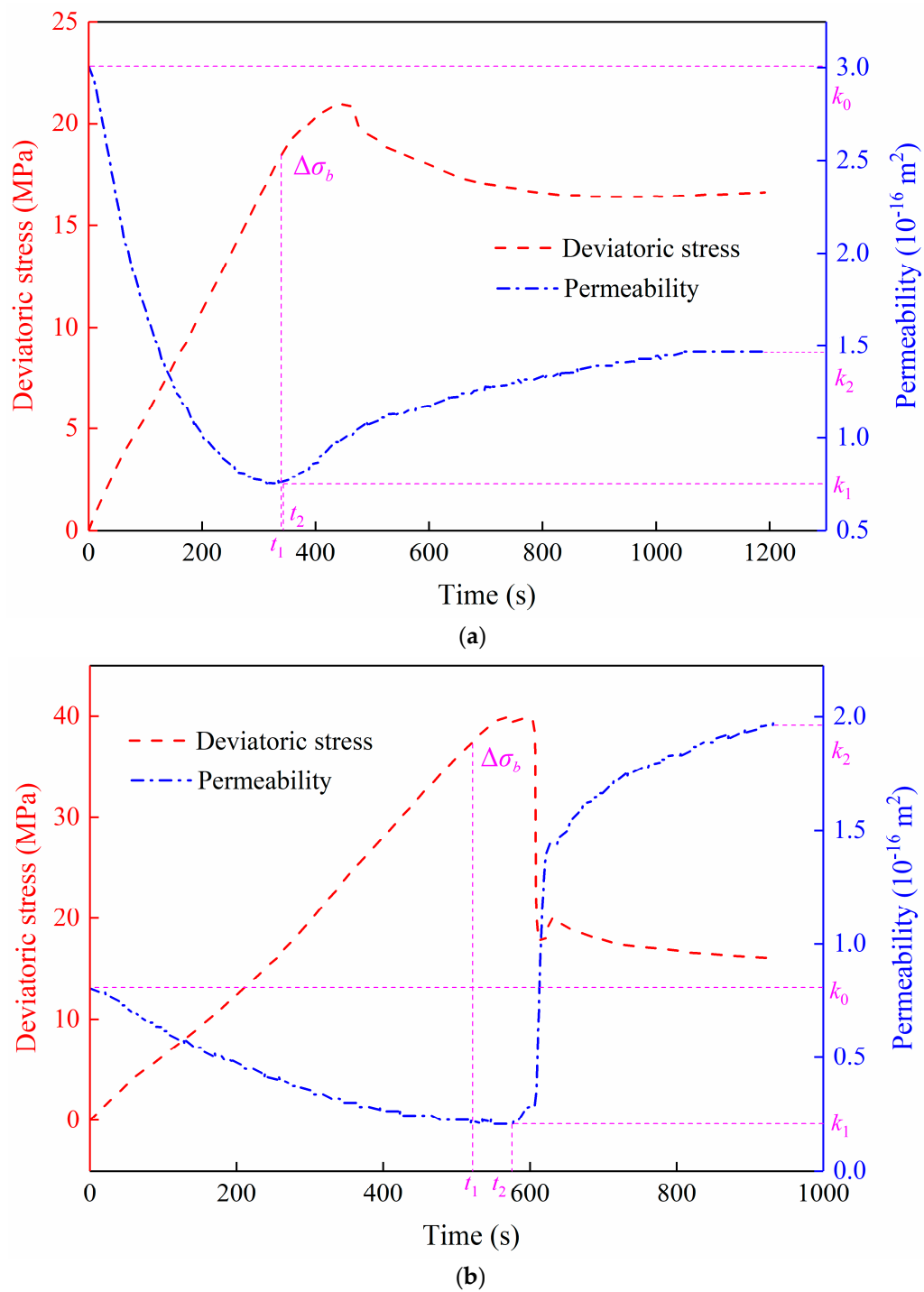


Figure 4. Stress-permeability-time curves of coal under triaxial compression. (a) tectonic coal and (b) intact coal.

Table 4. Critical permeabilities of tectonic and intact coal during each stage.

Coal Sample	k_0 (10^{-16} m^2)	k_1 (10^{-16} m^2)	k_2 (10^{-16} m^2)	k_1/k_0 (%)	k_2/k_0 (%)
Tectonic coal	3.01	0.75	1.47	24.9	48.8
Intact coal	0.80	0.21	1.96	26.3	245.0

The permeability recovery value after tectonic coal failure is very limited, even lower than that of intact coal, although its primary permeability is much higher than that of intact coal. On the contrary, the permeability recovery value after intact coal failure is more than twice of its primary permeability. The reasons may be that the original structure of tectonic coal was destroyed by tectonism, causing the coal to be severely crushed or even pulverized, and the particles can block the coal fractures after coal failure, hindering the recovery of coal permeability [9,28]. Considering the seepage lagging and recovery effect of tectonic and intact coal, the tectonic coal is appropriate to develop hydraulic flushing technology for permeability enhancement due to its high primary permeability and low permeability recovery after coal failure, while the intact coal is appropriate to develop hydraulic fracturing technology for permeability enhancement due to its low primary permeability and high permeability recovery after coal failure.

3.3. Permeability Sensitive Effect during Gas Depletion

Coal permeability is an important reservoir property during gas drainage which controls the gas drainage rate; thus, it is of significance to study the law of coal permeability during gas depletion. Figure 5 shows the relationships between effective stress, gas flow rate, and gas pressure during gas depletion. It is obvious that with gas depletion, the effective stress increases linearly with the decrease of gas pressure because the axial stress and confining stress are fixed. However, the gas flow rate decreases rapidly first and then slowly with the decrease of gas pressure, and the gas flow rate of tectonic coal is about one order of magnitude higher than that of intact coal. The fitting of the experimental data shows that the relationship between gas flow rate and gas pressure obeys a quadratic polynomial function, no matter the tectonic coal or intact coal, as shown in Table 5.

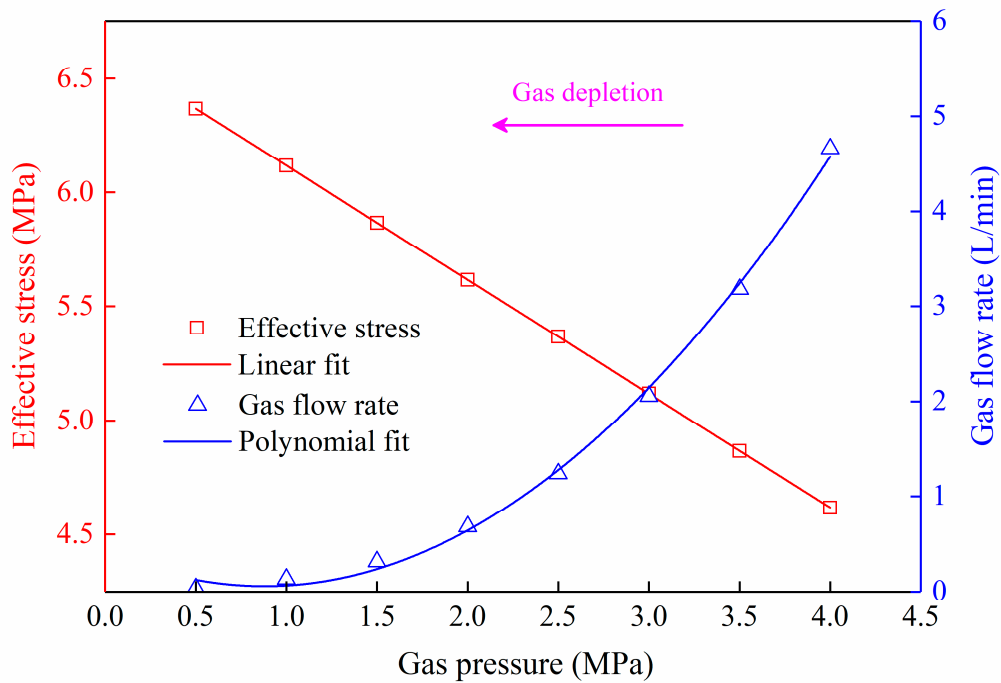
Table 5. Relationship between gas flow rate and gas pressure during gas depletion.

Coal Sample	Fitting Equation	R^2
Tectonic coal	$q = 0.4634p^2 - 0.8142p + 0.4154$	0.9979
Intact coal	$q = 0.038p^2 - 0.0465p + 0.0524$	0.9999

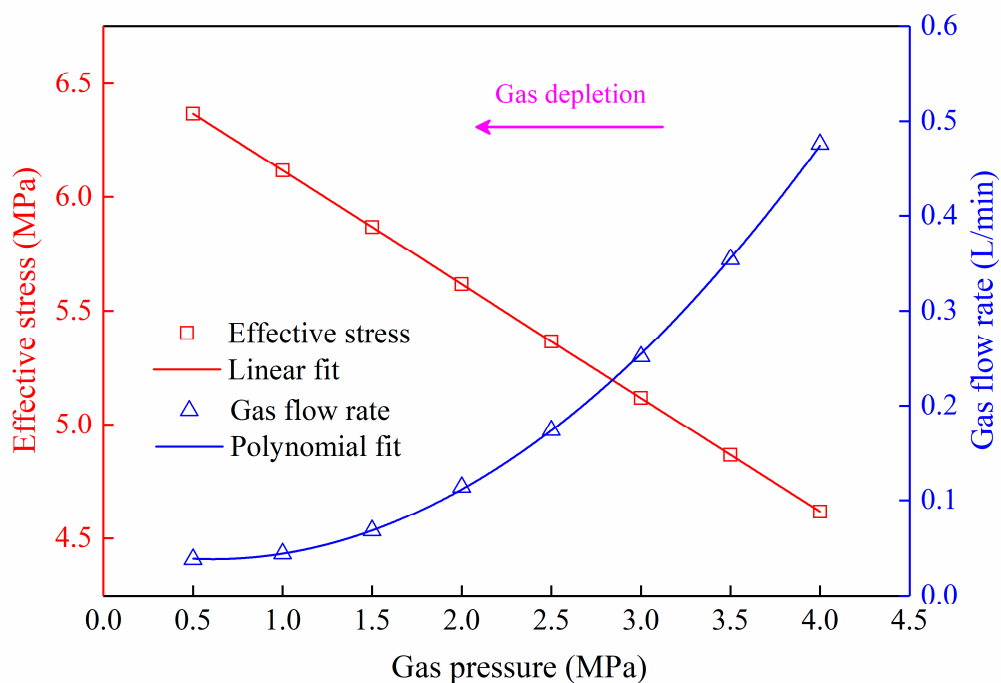
The permeability of coal is mainly controlled by its fracture system and affected by stress conditions and gas pressure [33]. Considering that the linear correlation between stress and gas pressure, only the curve of permeability evolution with gas pressure during gas depletion is plotted, as shown in Figure 6. It can be found that the permeability of tectonic coal has the maximum value of $5.409 \times 10^{-16} \text{ m}^2$ at 4.0 MPa, then reduces to $2.480 \times 10^{-16} \text{ m}^2$ at 1.0 MPa and recovers to $2.263 \times 10^{-16} \text{ m}^2$ at 0.5 MPa eventually. Accordingly, the permeability of intact has the maximum value of $0.564 \times 10^{-16} \text{ m}^2$ at 4.0 MPa, then reduces to $0.522 \times 10^{-16} \text{ m}^2$ at 2.0 MPa and recovers to $0.652 \times 10^{-16} \text{ m}^2$ at 0.5 MPa eventually. There are three differences between the permeability evolution of tectonic and intact coal. Firstly, the permeability drop ratio of tectonic coal from the maximum value to the minimum value (54.15%) is bigger than that of intact coal (7.45%), and the permeability recovery ratio of tectonic coal from the minimum value to the final value (5.36%) is smaller than that of intact coal (24.9%). Secondly, the rebound gas pressure of tectonic coal (1.0 MPa) is smaller than that of intact coal (2.0 MPa). Moreover, the permeability of tectonic coal is one order of magnitude larger than that of intact coal before the gas pressure drops to 2.0 MPa, and they become closer after that.

As we know, the effective stress increases continuously leading to a drop in coal permeability with gas depletion. Meanwhile, the shrinkage of coal matrix due to gas desorption will open the seepage pores and improve the coal permeability. At the same time, the Klinkenberg effect has an advantageous impact on gas seepage in gas reservoirs, especially in low permeability materials at finite gas pressure [34]. Considering the effective stress effects for permeability drop of tectonic and intact coal are close. It can be concluded that the matrix shrinkage effect and Klinkenberg effect for permeability rise of intact coal are more significant than that of tectonic coal. The low permeability of intact coal and the broken of tectonic coal may be the two principal reasons. Therefore, in tectonic

coal area, we should try to stabilize the gas extraction time at high gas pressure stage. While in intact coal area, we should increase the gas extraction time at low gas pressure stage and take permeability enhancement measures to reach the high and stable production of coalbed methane.



(a)



(b)

Figure 5. Effective stress-gas flow rate-gas pressure curves of coal during gas depletion. (a) tectonic coal; (b) intact coal.

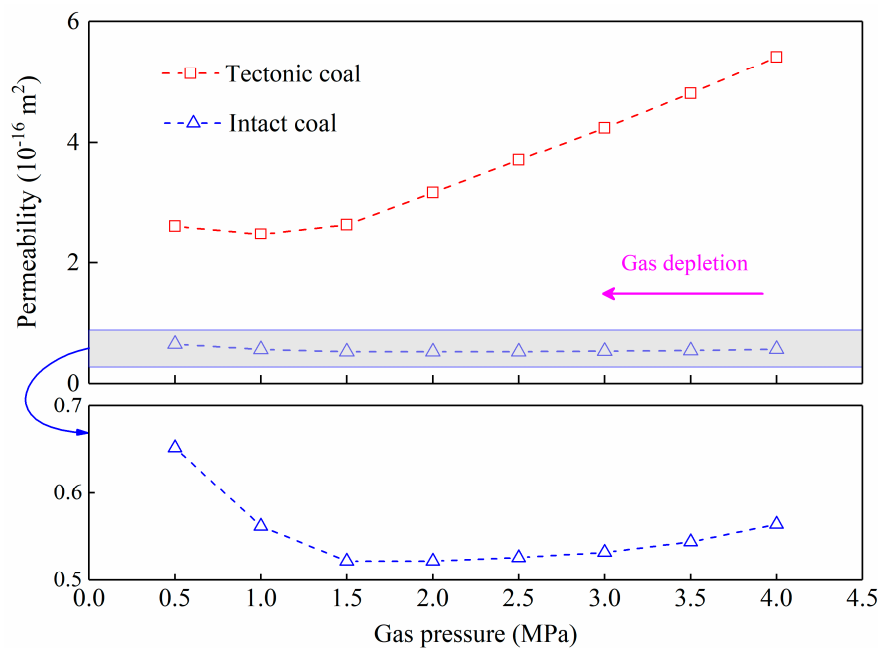


Figure 6. The evolution of coal permeability during gas depletion.

4. Conclusions

In this study, the triaxial compression and gas depletion experiments using both tectonic and intact coal were conducted. The mechanics and seepage characteristics of tectonic and intact coal under the coupling effect of stress and gas pressure were analyzed and compared. The key findings are summarized as follows.

1. The triaxial compression process of coal can be divided into four stages. The damage stress and peak stress of tectonic coal is only half that of intact coal, while their compaction stress or residual stress are almost the same. The deviatoric stress of intact coal during the post-destruction stage has a sharp drop while that of tectonic coal decreases slowly which shows an apparent strain softening behavior.
2. During the triaxial compression, the primary permeability and minimum permeability of tectonic coal are 3.76 times and 3.57 times that of intact coal. However, the permeability recovery value after intact coal failure is more than twice of its primary permeability, leading to that the residual permeability of tectonic is only 75.0% that of intact coal.
3. During the gas depletion, the permeability drop ratio of tectonic coal from the maximum value to the minimum value (54.15%) is bigger than that of intact coal (7.45%), and the rebound gas pressure of tectonic coal (1.0 MPa) is smaller than that of intact coal (2.0 MPa). In addition, the permeability of tectonic coal is one order of magnitude larger than that of intact coal before the gas pressure drops to 2.0 MPa, and they become closer after that.
4. The research results provide the reference and inspiration for the applications of coalbed methane recovery: the gas extraction time at high gas pressure stage should be stabilized in the tectonic coal area, while the gas extraction time at low gas pressure stage should be increased in the intact coal area. Moreover, the tectonic coal is suitable for hydraulic flushing technology while the intact coal is suitable for hydraulic fracturing technology in order to improve coal seam permeability and coalbed methane recovery.

Author Contributions: This article was completed by all authors. C.Z. and J.X. designed the experiments. C.Z. and S.P. performed the experiments. C.Z. and E.W. made the experimental analysis. All authors have read and agreed to the published version of the manuscript.

Funding: This work was supported by the National Natural Science Foundation of China (No. 51904293, No. 51874055), the National Science and Technology Major Project of China (No. 2016ZX05044-002), the Natural Science Foundation of Jiangsu Province (No. BK20190627), and the China Postdoctoral Science Foundation (No. 2019M661998).

Acknowledgments: The authors would like to thank the support of the laboratory and university.

Conflicts of Interest: The authors declare no conflict of interest.

References

1. Liu, Q.Q.; Chu, P.; Zhu, J.T.; Cheng, Y.P.; Wang, D.Y.; Lu, Y.F.; Liu, Y.Y.; Xia, L.; Wang, L. Numerical assessment of the critical factors in determining coal seam permeability based on the field data. *J. Nat. Gas Sci. Eng.* **2020**, *74*, 103098. [[CrossRef](#)]
2. Yan, F.Z.; Xu, J.; Peng, S.J.; Zou, Q.L.; Zhou, B.; Long, K.; Zhao, Z.G. Breakdown process and fragmentation characteristics of anthracite subjected to high-voltage electrical pulses treatment. *Fuel* **2020**, *275*, 117926. [[CrossRef](#)]
3. Fu, H.J.; Tang, D.Z.; Xu, T.; Xu, H.; Tao, S.; Li, S.; Yin, Z.Y.; Chen, B.L.; Zhang, C.; Wang, L.L. Characteristics of pore structure and fractal dimension of low-rank coal: A case study of Lower Jurassic Xishanyao coal in the southern Junggar Basin, NW China. *Fuel* **2017**, *193*, 254–264. [[CrossRef](#)]
4. Zhang, C.L.; Xu, J.; Peng, S.J.; Li, Q.X.; Yan, F.Z. Experimental study of drainage radius considering borehole interaction based on 3D monitoring of gas pressure in coal. *Fuel* **2019**, *239*, 955–963. [[CrossRef](#)]
5. Mavor, M.J.; Vaughn, J.E. Increasing coal absolute permeability in the San Juan basin fruitland formation. *SPE Reserv. Eval. Eng.* **1998**, *1*, 201–207. [[CrossRef](#)]
6. Moore, T.A. Coalbed methane: A review. *Int. J. Coal Geol.* **2012**, *101*, 36–81. [[CrossRef](#)]
7. Cheng, Y.P.; Pan, Z.J. Reservoir properties of Chinese tectonic coal: A review. *Fuel* **2020**, *260*, 116350. [[CrossRef](#)]
8. Schweinfurth, S.P. *Coal—A Complex Natural Resource: An Overview of Factors Affecting Coal Quality and Use in the United States*; US department of the interior, US Geological Survey: Washington, DC, USA, 2003.
9. Wang, E.; Shao, Q.; Han, S. Mechanics analysis of normal fault formation and control of structure coal. *Coal Sci. Technol.* **2009**, *37*, 104–113.
10. Jin, K.; Cheng, Y.P.; Ren, T.; Zhao, W.; Tu, Q.; Dong, J.; Hu, B. Experimental investigation on the formation and transport mechanism of outburst coal-gas flow: Implications for the role of gas desorption in the development stage of outburst. *Int. J. Coal Geol.* **2018**, *194*, 45–58. [[CrossRef](#)]
11. Lu, S.Q.; Cheng, Y.P.; Li, W.; Wang, L. Pore structure and its impact on CH₄ adsorption capability and diffusion characteristics of normal and deformed coals from Qinshui Basin. *Int. J. Oil Gas Coal Technol.* **2015**, *10*, 76–84. [[CrossRef](#)]
12. Jiang, B.; Ju, Y.W. Tectonic coal structure and its petrophysical features. *Nat. Gas Ind.* **2004**, *24*, 27–36.
13. Li, W.; Liu, H.; Song, X. Multifractal analysis of Hg pore size distributions of tectonically deformed coals. *Int. J. Coal Geol.* **2015**, *144*, 138–152. [[CrossRef](#)]
14. Skoczylas, N.; Dutka, B.; Sobczyk, J. Mechanical and gaseous properties of coal briquettes in terms of outburst risk. *Fuel* **2014**, *134*, 45–52. [[CrossRef](#)]
15. Quosay, A.A.; Knez, D.; Ziaja, J. Hydraulic fracturing: New uncertainty based modeling approach for process design using Monte Carlo simulation technique. *PLoS ONE* **2020**, *15*, 0236726. [[CrossRef](#)] [[PubMed](#)]
16. Quosay, A.A.; Knez, D. Sensitivity analysis on fracturing pressure using Monte Carlo simulation technique. *Oil Gas Eur. Mag.* **2016**, *42*, 140–144.
17. Chaturvedi, T.; Schembre, J.M.; Kovscek, A.R. Spontaneous imbibition and wettability characteristics of Powder River Basin coal. *Int. J. Coal Geol.* **2009**, *77*, 34–42. [[CrossRef](#)]
18. Zhang, C.; Tu, S.H.; Zhang, L. Pressure-relief and methane production performance of pressure relief gas extraction technology in the longwall mining. *J. Geophys. Eng.* **2017**, *14*, 77–89. [[CrossRef](#)]
19. Zhang, C.; Zhang, L. Permeability characteristics of broken coal and rock under cyclic loading and unloading. *Nat. Resour. Res.* **2019**, *28*, 1055–1069. [[CrossRef](#)]
20. Chen, Y.X.; Xu, J.; Chu, T.X. Experimental study on the influence of moisture content during gas depressurization extraction. *Adv. Mater. Sci. Eng.* **2019**, 9804825. [[CrossRef](#)]

21. Zhang, C.L.; Xu, J.; Peng, S.J.; Zhang, X.L.; Liu, X.R.; Chen, Y.X. Dynamic evolution of coal reservoir parameters in CBM extraction by parallel boreholes along coal seam. *Transp. Porous Media*. **2018**, *124*, 325–343. [[CrossRef](#)]
22. Zhang, C.L.; Xu, J.; Wang, E.Y.; Peng, S.J. Experimental study on the gas flow characteristics and pressure relief gas drainage effect under different unloading stress paths. *Geofluids* **2020**, 8837962. [[CrossRef](#)]
23. Yin, G.Z.; Jiang, C.B.; Xu, J. Geomechanical and flow properties of coal from loading axial stress and unloading confining pressure tests. *Int. J. Rock Mech. Min.* **2015**, *76*, 155–161. [[CrossRef](#)]
24. Yin, G.; Li, M.; Jiang, C.B.; Xu, J.; Li, W.P. Mechanical behavior and permeability evolution of gas infiltrated coals during protective layer mining. *Int. J. Rock Mech. Min.* **2015**, *80*, 292–301. [[CrossRef](#)]
25. Liu, T.; Liu, S.M.; Lin, B.Q.; Fu, X.H.; Zhu, C.J.; Yang, W.; Zhao, Y. Stress response during in-situ gas depletion and its impact on permeability and stability of CBM reservoir. *Fuel* **2020**, *266*, 117083. [[CrossRef](#)]
26. Lu, S.; Cheng, Y.P.; Qin, L.M.; Li, W.; Zhou, H.X.; Guo, H.J. Gas desorption characteristics of the high-rank intact coal and fractured coal. *Int. J. Min. Sci. Technol.* **2015**, *25*, 819–844. [[CrossRef](#)]
27. Dong, J.; Cheng, Y.P.; Hu, B.; Hao, C.M.; Tu, Q.Y.; Liu, Z.D. Experimental study of the mechanical properties of intact and tectonic coal via compression of a single particle. *Powder Technol.* **2018**, *325*, 412–419. [[CrossRef](#)]
28. Liu, R.; He, Y.; Zhao, Y.F.; Jiang, X.; Ren, S. Statistical analysis of acoustic Emission in uniaxial compression of tectonic and non-tectonic coal. *Appl. Sci.* **2020**, *10*, 3555. [[CrossRef](#)]
29. Yin, G.Z.; Jiang, C.B.; Xu, J.; Guo, L.S.; Peng, S.J.; Li, W.P. An experimental study on the effects of water content on coalbed gas permeability in ground stress fields. *Transp. Porous Media* **2012**, *94*, 87–99. [[CrossRef](#)]
30. Zhang, C.L.; Xu, J.; Peng, S.J.; Li, Q.X.; Yan, F.Z.; Chen, Y.X. Dynamic behavior of gas pressure and optimization of borehole length in stress relaxation zone during coalbed methane production. *Fuel* **2018**, *233*, 816–824. [[CrossRef](#)]
31. Li, B.B.; Ren, C.H.; Wang, Z.H.; Li, J.H.; Yang, K.; Xu, J. Experimental study on damage and the permeability evolution process of methane-containing coal under different temperature conditions. *J. Petrol. Sci. Eng.* **2020**, *184*, 106509. [[CrossRef](#)]
32. Yin, G.Z.; Jiang, C.B.; Wang, J.G.; Xu, J. Combined effect of stress, pore pressure and temperature on methane permeability in anthracite coal: An experimental study. *Transp. Porous Media* **2013**, *100*, 1–16. [[CrossRef](#)]
33. Cui, X.J.; Bustin, R.M. Volumetric strain associated with methane desorption and its impact on coalbed gas production from deep coal seams. *AAPG Bull.* **2005**, *89*, 1181–1202. [[CrossRef](#)]
34. Tao, Y.Q.; Liu, D.; Xu, J.; Peng, S.J.; Nie, W. Investigation of the klinkenberg effect on gas flow in coal matrices: A numerical study. *J. Nat. Gas Sci. Eng.* **2016**, *30*, 237–247. [[CrossRef](#)]

Publisher’s Note: MDPI stays neutral with regard to jurisdictional claims in published maps and institutional affiliations.



© 2020 by the authors. Licensee MDPI, Basel, Switzerland. This article is an open access article distributed under the terms and conditions of the Creative Commons Attribution (CC BY) license (<http://creativecommons.org/licenses/by/4.0/>).